

## NUCLEAR RESONANT SCATTERING AT HIGH PRESSURE AND HIGH TEMPERATURE

JIYONG ZHAO<sup>a,\*</sup>, WOLFGANG STURHAHN<sup>a</sup>, JUNG-FU LIN<sup>b</sup>, GUOYIN SHEN<sup>c</sup>,  
ERCAN E. ALP<sup>a</sup> and HO-KWANG MAO<sup>b</sup>

<sup>a</sup>Advanced Photon Source, Argonne National Laboratory, 9700 South Cass Avenue, Argonne, IL 60439, USA; <sup>b</sup>Geophysical Laboratory, Carnegie Institution of Washington, Washington, DC 20015, USA; <sup>c</sup>Consortium for Advanced Radiation Sources, The University of Chicago, Chicago, IL 60637, USA

(Received ???)

We introduce the combination of nuclear resonant inelastic X-ray scattering and synchrotron Mössbauer spectroscopy with the laser-heated diamond anvil cell technique for studying magnetic, elastic, thermodynamic, and vibrational properties of materials under high pressures and high temperatures. An Nd:YLF laser, operating in continuous donut mode (TEM<sub>01</sub>), has been used to heat samples inside a diamond anvil cell from both sides. Temperatures of the laser-heated sample are measured by means of spectral radiometry and by the detailed balance principle of the energy spectra. The temperature measured by the detailed balance principle is in very good agreement with values determined from the thermal radiation spectra fitted to the Planck radiation function up to 1700 K. Nuclear resonant scattering on <sup>57</sup>Fe-containing materials (i.e., Fe, FeO, Fe<sub>2</sub>O<sub>3</sub>) has been studied up to 2500 K and 100 GPa. A detailed description of the laser-heating optics, temperature determination, the X-ray monochromatization, and the X-ray focusing optics is given in this article.

**Keywords:** Laser heating; Diamond anvil cell; Nuclear resonant scattering; Synchrotron radiation

### INTRODUCTION

Nuclear resonant scattering (NRS) techniques, including nuclear resonant inelastic X-ray scattering (NRIXS) [1, 2] and synchrotron Mössbauer spectroscopy (SMS) [3], at highly brilliant third generation synchrotron radiation light sources have been successfully applied to study materials under high pressures in diamond anvil cells (DAC) [4–6]. The NRIXS technique provides a direct probe of the phonon density of states (DOS) of a resonant isotope, whereas the SMS technique probes the magnetic properties of a sample [7, 8]. These techniques have been used to study elastic, magnetic, thermodynamic, and vibrational properties of hexagonal close-packed (hcp) Fe up to 153 GPa at 300 K [4], Fe to 29 GPa at 920 K by wire heating [9], and Fe-Ni, Fe-Si, and Fe-S alloys [10, 11], providing important information on the physical properties of Fe and its alloys, such as compressional wave velocity ( $V_P$ ), shear wave velocity ( $V_S$ ), and shear modulus ( $G$ ) under high pressure and high temperature conditions. The NRS techniques have become unique and important tools to study the lattice

---

\* Corresponding author. Tel.: +1-630-252-9195; Fax: +1-630-252-0161; E-mail: jzhao@anl.gov

dynamics and hyperfine interactions of materials under high pressures. These results have provided valuable information in understanding physical properties of materials in deep planetary interiors.

On the other hand, the laser-heated diamond-anvil cell (LHDAC) technique is a unique static method to generate extreme pressures ( $P > 100$  GPa) and temperatures ( $T > 3000$  K). Since the birth of the LHDAC in the late 1960s [12, 13], the LHDAC technique has been widely used in X-ray diffraction, melting point studies, phase equilibrium studies, and chemical analyses of quenched samples [14–20]. These studies provided data on phase diagram, equation of state, elasticity, composition, and melting curve of planetary materials. The combination of NRS and LHDAC techniques would extend our scope in studying materials at extreme conditions. Important physical properties, such as magnetic, thermodynamic, and elastic properties of materials under high pressures and temperatures simultaneously, can be studied with this development, which are of great importance in high-pressure material science and geophysics.

In the past two decades, techniques using the LHDAC have been advanced in heating capability, temperature measurement, and other related techniques [19, 20]. However, the combination of the LHDAC and NRS studies is not straightforward, mostly due to long counting times for NRS experiments. The typical collecting time for a meaningful NRIXS spectrum at the 3-ID beamline of the advanced photon source (APS) is at least 4–6 h. So far, most LHDAC systems are only required to provide stable heating conditions on the order of minutes for *in situ* X-ray diffraction experiments. It is thus more challenging to design an LHDAC system for NRS application. Furthermore, the use of a high-resolution monochromator with meV bandwidth and Avalanche photodiode (APD) timing detectors in NRS experiments requires a stable thermal environment in the experimental hutch and around the DAC. In particular, heated DAC has to be thermally insulated to minimize the effects on the environment.

Here, we describe a system to perform NRIXS and SMS in the LHDAC at beamline 3-ID of the APS, Argonne National Laboratory.

## THE LASER-HEATED DIAMOND ANVIL CELL SYSTEM

The schematic diagram of a double-sided LHDAC system at 3-ID is shown in Figure 1. The detailed designs and experimental procedures of the laser-heating system are similar to a system installed at GSECARS of the APS [19] with some modifications to accommodate the special requirements of the NRS experiments. In order to make the system compact, a two-tier structure is used for the system. The laser and most of the laser optics are located on the top tier, whereas the DAC and X-ray optics are located on the bottom tier (shown in Fig. 2). The laser is guided through two holes of the top tier and focused on the sample in a DAC on the bottom tier. An Nd:YLF laser ( $1.053 \mu\text{m}$ ) with a maximum power of 80 W operating in continuous donut mode ( $\text{TEM}_{01}$ ) is located at the top tier and is used to heat the sample in a DAC from both sides. The output power of the laser is controlled by regulating its linear polarization of the laser radiation with a wave plate (WP1) and a polarizing beam splitter (BS1). The size of the laser beam is controlled by a beam expander (BE). A photodiode (PIN) behind the laser mirror (M2) is used to monitor the output power of the laser. The laser beam is then split into two beams by the second set of wave plate and polarizing beam splitter (WP2 and BS2), which are also used to balance the laser power between the upstream and the downstream beam. The laser beams are guided by the mirror (M2) through holes on the supporting structure of the top tier to the bottom tier. The laser

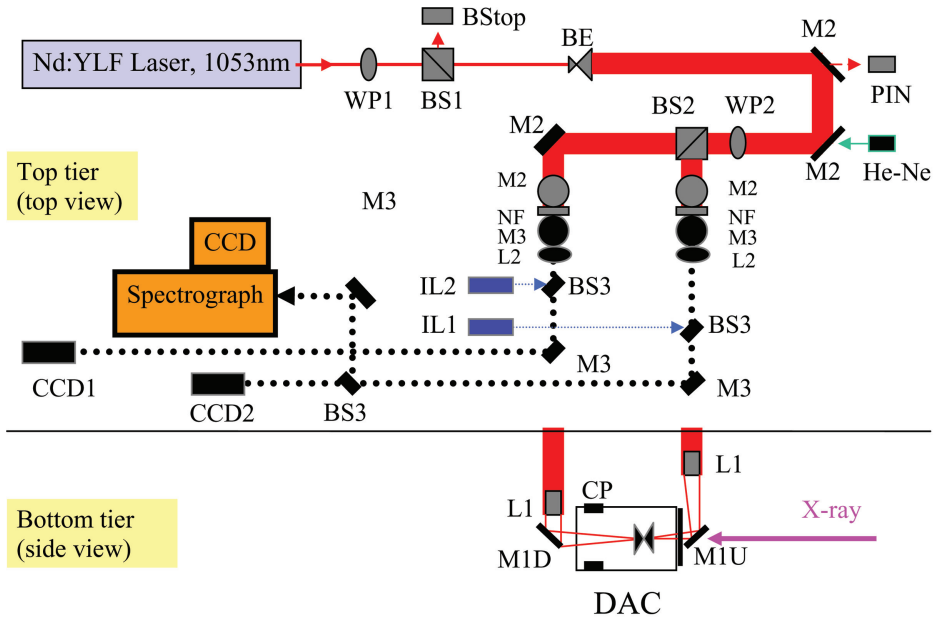


FIGURE 1 Schematic of the double-sided LHDAC system at 3-ID, APS. WP1, WP2: wave plate; BS1, BS2: polarizing cube beam splitter; BS3: 50/50 neutral beam splitter; BStop: water-cooled beam stop; BE: zoom beam expander; PIN: photodiode; M1: beryllium laser mirror coated with gold or carbon mirror coated with silver; M2: dichroic mirror reflecting ( $>99\%$ ) vertical polarized laser beam at 1053 nm; M3: Al-coated mirror; L1: apochromatic objective lens with focal length of 100 mm; L2: achromatic lens with 1000 mm focal length; NF: notch filter; CCD1 and CCD2: CCD cameras; CCD-spectrograph: spectrograph and CCD for temperature measurement; He-Ne: alignment laser; IL1 and IL2: illuminators.

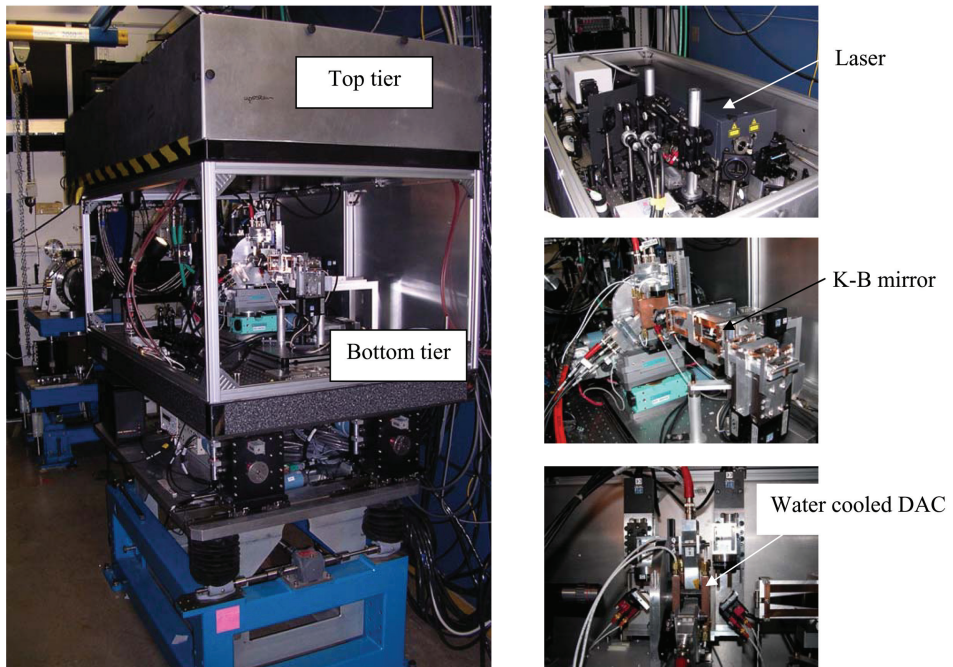


FIGURE 2 LHDAC system at 3-ID, APS.

beams are focused by two apochromatic objective lenses ( $L1, f = 100$  mm). An upstream beryllium mirror coated with gold (M1U) and a downstream carbon mirror coated with silver (M1D) are used to guide the laser beam onto the sample in a DAC. These two mirrors also reflect the images of samples from both sides back to the top tier to two charged-coupled-devices (CCD), CCD1 and CCD2. The thermal radiation from the upstream of the heated sample is reflected back to the top tier by M1U for spectral radiometric temperature measurements using a spectrograph and a CCD. A He-Ne laser is aligned to be coaxial with the Nd:YLF laser and serves as an alignment laser. Two achromatic lenses ( $L2, f = 1000$  mm) are used to focus the sample images to CCD cameras. For the upstream beam, a 50/50 beam splitter (BS3) is used to reflect part of the radiation into the spectrograph. In order to minimize the influence on the detector and high-resolution monochromator (HRM), the laser, the beam stop, and the DAC are water cooled. The DAC is attached to copper plates cooled by water ( $10$  °C). The temperature of the DAC stays below  $310$  K during data collection, which ensures mechanical stability.

The sample is loaded in a drilled hole in a Be gasket with NaCl or KCl on both sides to act as thermal insulator and pressure medium. The use of a beryllium gasket insures low absorption of the Fe K-fluorescence radiation. Small ruby chips are used as an internal pressure calibrant.

The laser beam size on the sample is adjusted to be around  $40$   $\mu\text{m}$ , so that the heating spot is bigger than the X-ray beam size ( $6$   $\mu\text{m} \times 6$   $\mu\text{m}$ ) but smaller than the sample size ( $50$ – $100$   $\mu\text{m}$  in diameter). After the system spectral response was calibrated using a reference with known radiance, gray-body temperatures were determined by fitting the thermal radiation spectrum between  $670$  and  $830$  nm to the Planck radiation function [19]. In addition to this spectral radiometric method, average temperatures of the laser-heated sample are determined by detailed balance principle of the energy spectra obtained from NRIXS [21].

## X-RAY OPTICS AND DETECTORS

Figure 3 shows the schematic setup of the NRS experiment. The insertion devices at 3-ID consist of two  $2.7$ -cm period undulators with a total length of  $4.5$  m. These devices produce  $14.4$ -keV X-rays in the first harmonic. The high heat-load monochromator consists of two flat diamonds ( $1\ 1\ 1$ ) in a  $(+, -)$  arrangement, giving an energy adjustable range of  $7$ – $28$  keV. The diamonds are indirectly cooled by water. One of the major components

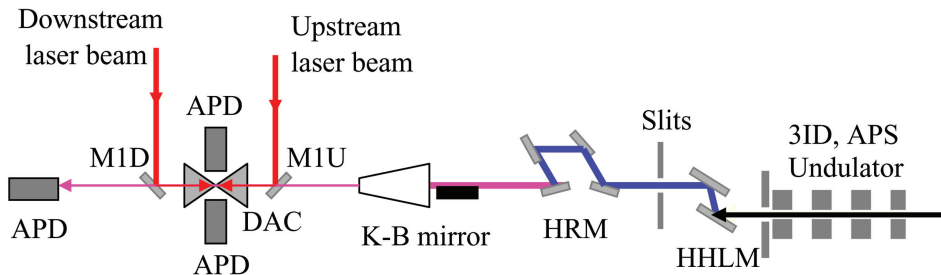


FIGURE 3 Experimental setup for NRIXS under high pressure and high temperature. HHLM: diamond high-heat-load monochromator; HRM: high-resolution monochromator; M1U and M1D: laser mirrors; DAC: diamond anvil cell; APD: Avalanche photodiode detector. The X-ray from the undulator is monochromatized by HHLM and HRM, focused by the K-B mirror, impinging on the sample in a DAC with a beam size of  $6$   $\mu\text{m}$  in both dimensions and energy bandwidth of  $1$  meV. The signal is collected by APDs.

for NRS studies is the HRM. Various HRMs have been built at 3-ID for experiments with  $^{83}\text{Kr}$  (9.4 keV),  $^{161}\text{Dy}$  (25.7 keV),  $^{151}\text{Eu}$  (21.5 keV),  $^{119}\text{Sn}$  (23.9 keV), and  $^{57}\text{Fe}$  (14.4 keV) isotopes [22]. In the case of the  $^{57}\text{Fe}$  isotope, the currently used HRM consists of four silicon single crystals in two weak-link assemblies, one using a pair of asymmetrically cut Si (4 0 0) and the other using a pair of asymmetrically cut Si (10 6 4) reflections [23]. The HRM produces a 1-meV energy bandwidth, as shown in Figure 4. The environmental temperature change in the experimental hutch is less than 20 mK over hours and 50 mK over days, which gives a stable condition for the HRM.

As the sample size is typically around 50–100  $\mu\text{m}$  and the laser beam is about 40  $\mu\text{m}$  in LHDAC experiments, a microfocused X-ray beam around 10  $\mu\text{m}$  in diameter is needed. This is achieved by using a pair of elliptically bent mirrors [Kirkpatrick–Baez (K–B) configuration], with a bending mechanism described earlier [24]. Two well-polished glass (Zerodur) substrates with a rhodium coating (thickness of 1200 Å) over a chromium binding layer (50 Å) are used to focus the X-ray beam. The size of the mirror is 200 mm (horizontal) by 100 mm (vertical). The mirror is located 35 m from the X-ray source. The vertical and horizontal acceptances of the mirror at 14.4 keV (the incident angle is 4 mrad) are 300  $\mu\text{m}$  and 700  $\mu\text{m}$ , respectively. The reflectivity of each mirror is about 85%. The beam size at the focusing spot was measured by scanning a knife (Si coated with Cr) edge across the X-ray beam in both horizontal and vertical directions while collecting Cr K-florescence with a Si(Li) detector (Fig. 5). The full width at half maximum (FWHM) in both directions is  $\sim 6\text{--}7\ \mu\text{m}$ . The photon flux at 14.4 keV at the focusing spot is about  $10^9$  photons/s with a 1-meV energy bandwidth.

Three APDs are used to collect the NRIXS signals. These detectors are placed as close to the sample as possible. A fourth APD is used to detect forward scattering, either to measure the resolution function during the NRIXS experiment or to measure the SMS time spectrum.

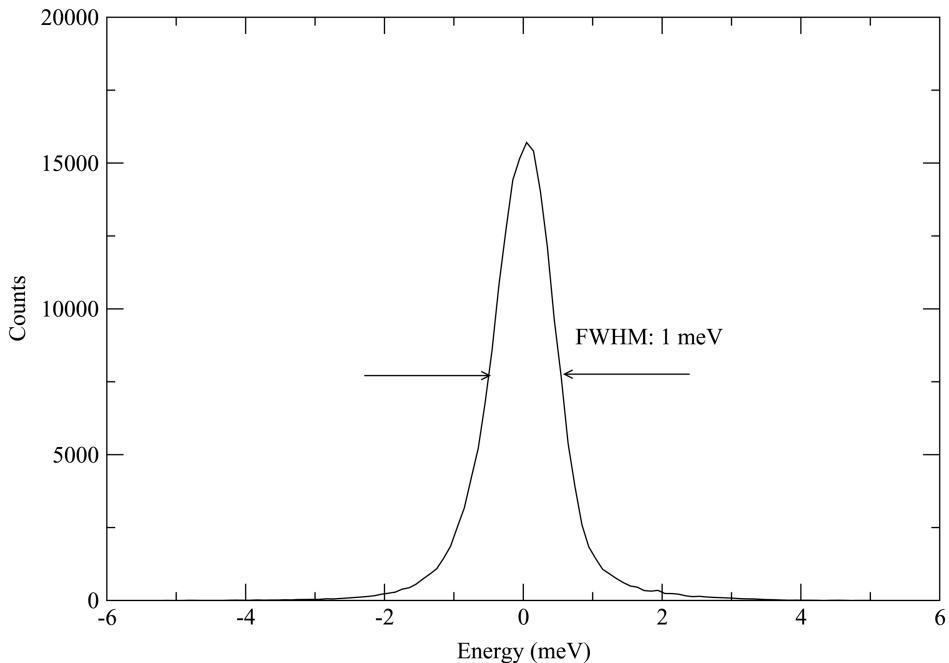


FIGURE 4 Resolution function of the HRM for  $^{57}\text{Fe}$  resonance with an energy bandwidth of 1 meV. The resolution is measured using the SMS signal of  $^{57}\text{Fe}$ .

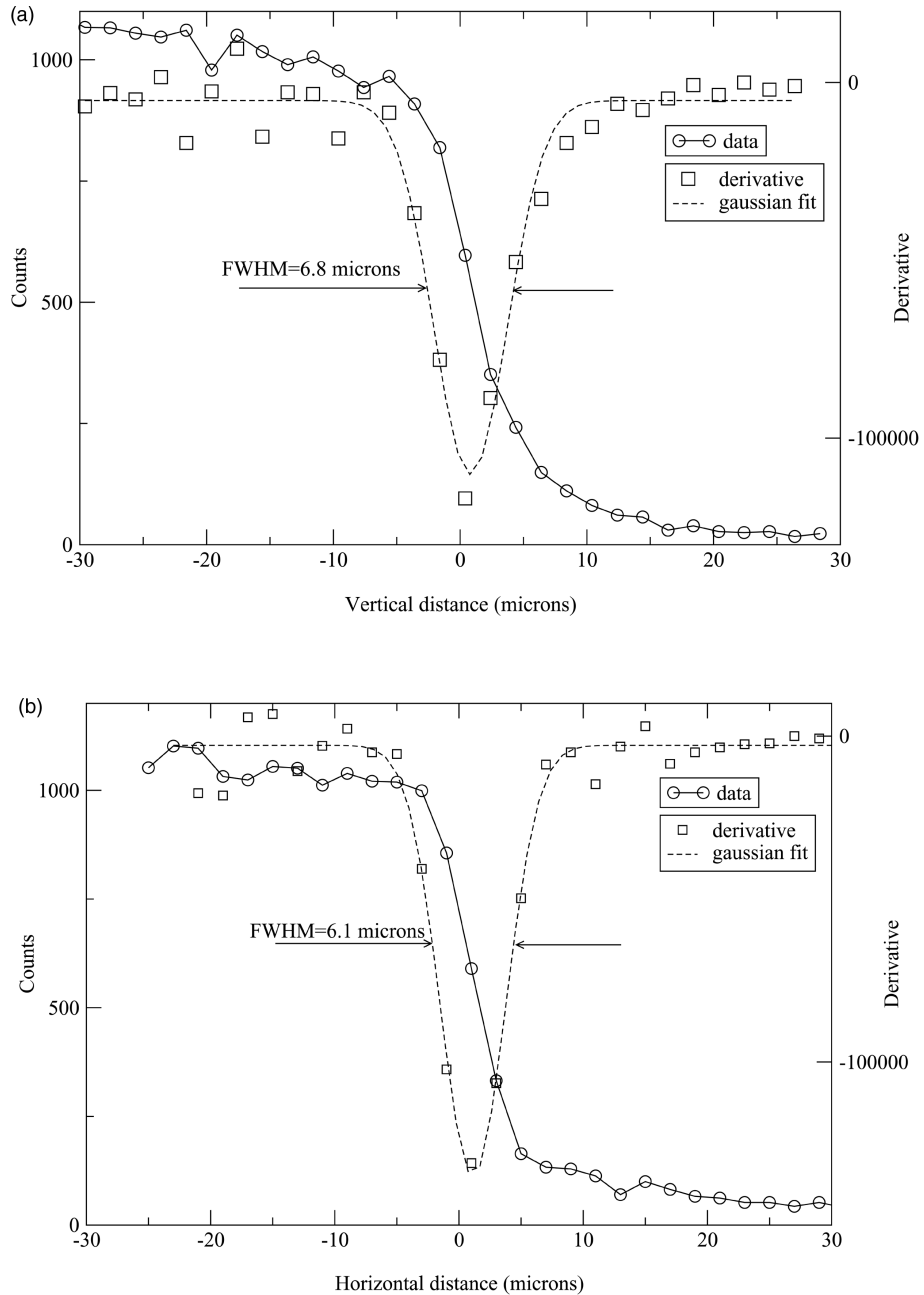


FIGURE 5 Knife-edge scan measuring the X-ray beam size along (a) vertical and (b) horizontal directions. The curves with open circles (left axis) are Cr K-edge fluorescence measured by a Si(Li) detector while scanning the Cr sharp edge over a focusing spot. The solid curves (right axis) are derivatives of the above-measured curves, which give the beam size of the focusing spot. The full width at half maximum (FWHM) is  $6.8 \mu\text{m}$  (V)  $\times$   $6.1 \mu\text{m}$  (H).

As the semiconductor diode is very sensitive to the temperature changes, the temperature rise during sample heating is limited to a few degrees by efficiently cooling the DAC. The temperature of the sample around 1500 K fluctuates less than 150 K over more than 10 h, allowing sufficiently stable conditions to collect NRIXS spectra.

**EXPERIMENTAL RESULTS**

The system has been used to study SMS and NRIXS of  $^{57}\text{Fe}$ -enriched materials such as Fe, FeO, and  $\text{Fe}_2\text{O}_3$  up to 100 GPa and 2500 K. As an example, Figure 6(a) shows energy spectra

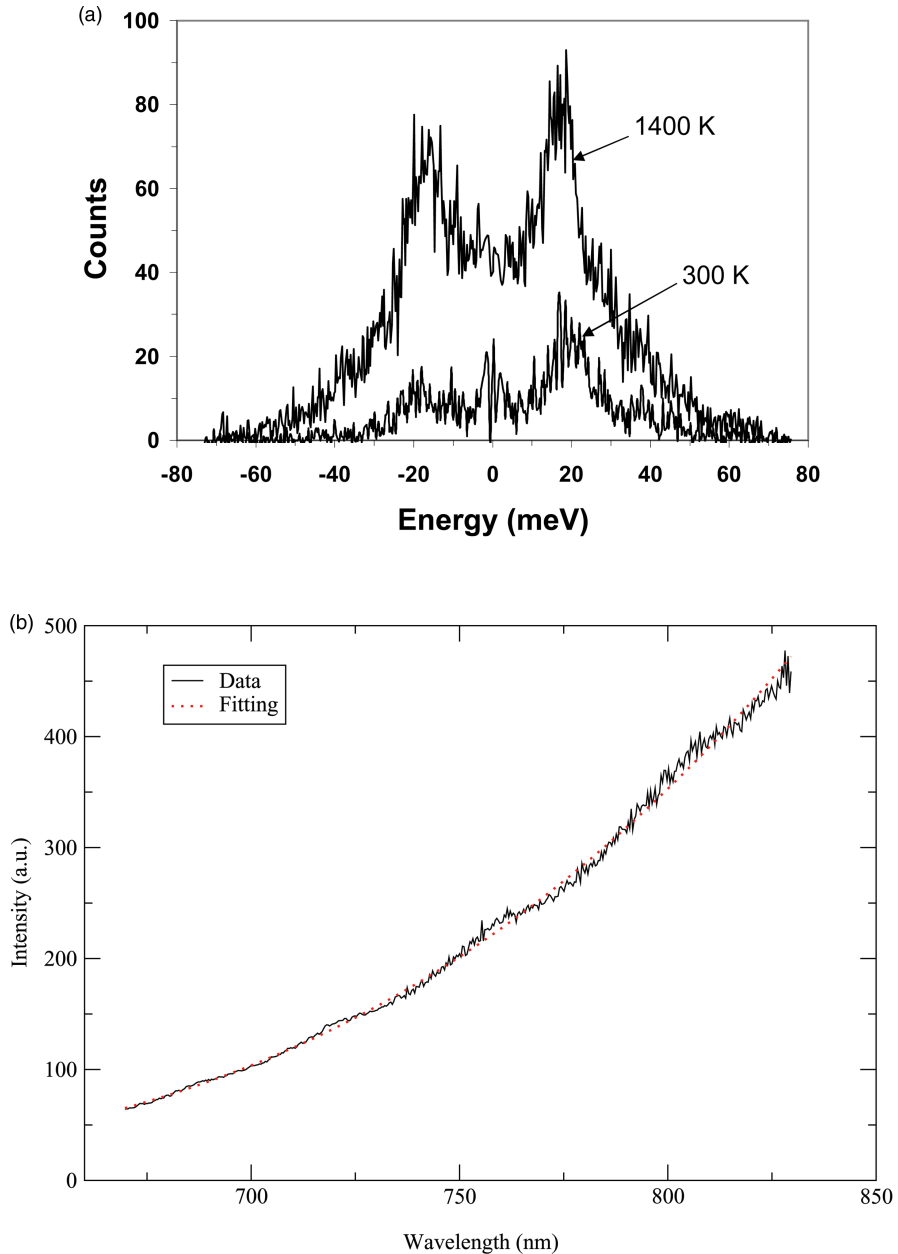


FIGURE 6 (a) Energy spectra of hematite at 300 and 1400 K and at a pressure of 24 GPa. The elastic peak at zero energy (corresponding to  $^{57}\text{Fe}$  nuclear resonant energy) has been removed. The counting time for each spectrum was about 10 h. Negative/positive energies indicate net phonon annihilation/creation. The asymmetry of these spectra was used to determine the average temperature of the laser-heated sample. (b) Thermal radiation spectrum (solid line) measured by spectral radiometry. The dotted line is the fitting by Planck radiation function.

of  $^{57}\text{Fe}_2\text{O}_3$  (with elastic peak being removed) at 300 and 1400 K. We have measured temperatures of the laser-heated sample by two different methods: spectral radiometry [19, 25] and temperature-dependent intensity asymmetry of the NRIXS spectra based on the detailed balance principle [9, 21]. In Figure 6(a), the side band at positive energy represents phonon creation, whereas the side band at negative energy arises from phonon annihilation. The intensity ratio of phonon creation to phonon annihilation is low at 300 K; the intensity imbalance is reduced with increasing temperature due to the rising thermal population of the upper energy level of the phonons. The asymmetry of the NRIXS spectra is independent of sample properties other than temperature and is given by the Boltzmann factor,  $\exp[-E/k_{\text{B}}T]$  with the Boltzmann constant  $k_{\text{B}}$ , temperature  $T$ , and energy  $E$  [26]. Therefore, the intensity ratio is given by

$$\frac{I(E)}{I(-E)} = \exp^{E/k_{\text{B}}T}, \quad (1)$$

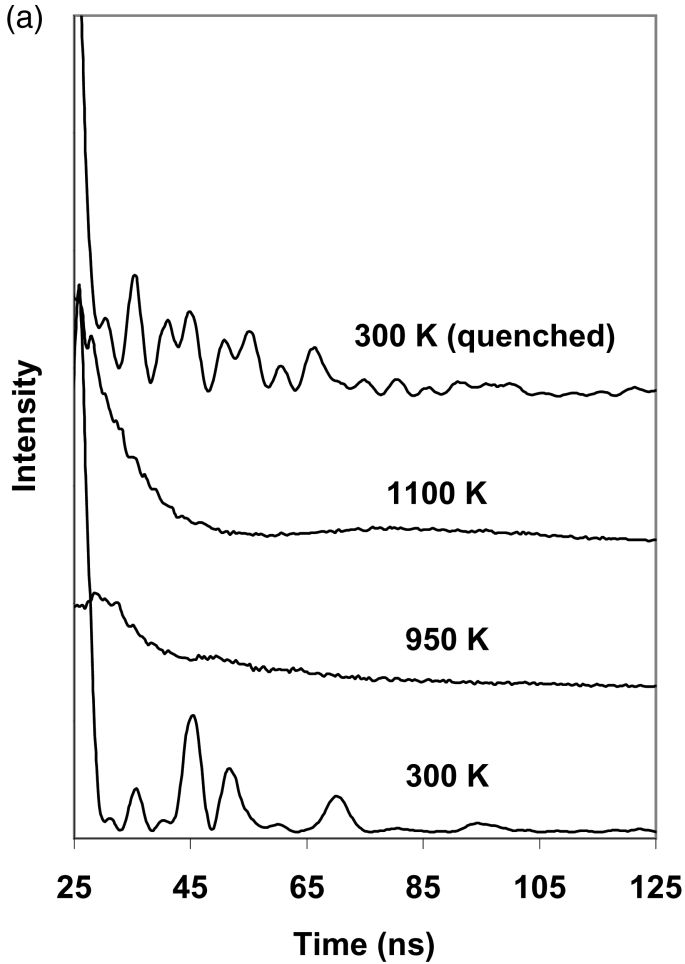


FIGURE 7 SMS time spectra of  $\text{Fe}_2\text{O}_3$  at (a) 10 GPa and (b) 24 GPa at different temperatures upon laser heating. Fast oscillations of the time spectrum (*i.e.*, 300 K, 300 K quenched in both (a) and (b)) originate from the nuclear level splitting, whereas the flat feature (*i.e.*, 950 and 1100 K in (a) and 900, 1200, and 1400 K in (b)) indicates nonmagnetic phase.



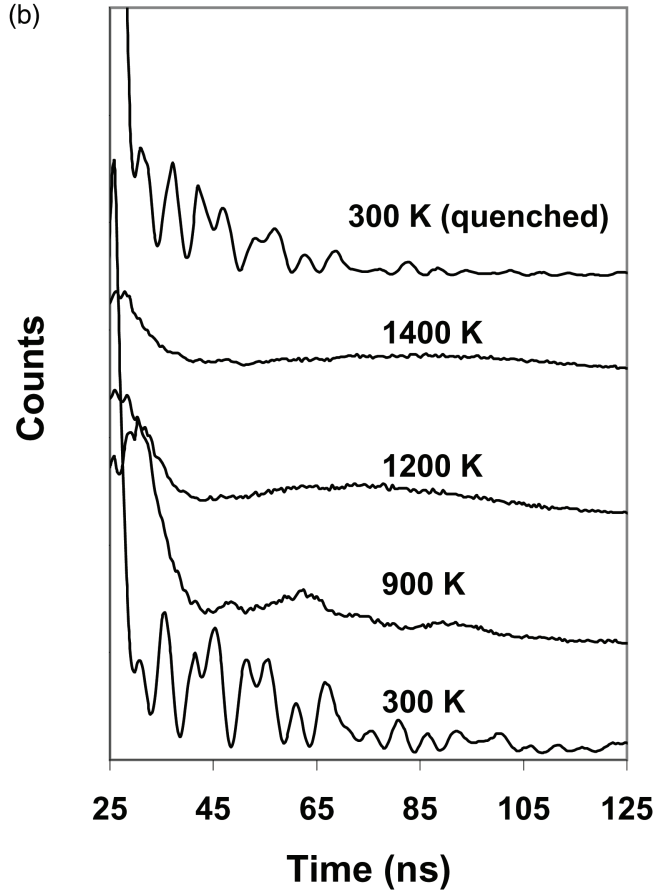


FIGURE 7 Continued.

where  $I(E)$  is the intensity of the phonon creation and  $I(-E)$  is the phonon annihilation. Each pair of measured intensities  $I(\pm E)$ , where  $E = 0$  corresponds to the nuclear transition energy of 14.4125 keV, gives a temperature value. The average temperature of the laser-heated sample is then determined by integrating all energy pairs from the energy range of 5–70 meV using the following equation:

$$\int I(E) dE = \int \exp^{E/k_B T} I(-E) dE. \quad (2)$$

The average so determined gives the sample temperature within the statistical accuracy of the spectra, which is 5–10% in our case. The temperature ( $1400 \pm 100$  K) is obtained from this method for the spectrum in Figure 6(a).

Figure 6(b) shows the thermal radiation spectrum measured by spectral radiometry. Temperatures are determined by fitting the thermal radiation spectrum between 670 and 830 nm to the Planck radiation function [19]. An average temperature over the heating spot is obtained as  $1360 \pm 120$  K. The temperature is in very good agreement with the values determined from the NRIXS spectrum.

Figure 7 shows SMS time spectra of  $^{57}\text{Fe}_2\text{O}_3$  at (a) 10 GPa and (b) 24 GPa upon laser heating. It shows that  $^{57}\text{Fe}_2\text{O}_3$  undergoes a magnetic to nonmagnetic transition above 900 K for both pressures from a room-temperature magnetic state to a high-temperature nonmagnetic state.

## DISCUSSION

The current LHDAC system at 3-ID was used successfully for both NRIXS and SMS studies. The temperature of the DAC body is stable within several degrees during the heating due to efficient water cooling. Sample temperatures of up to 2500 K for SMS studies and of 1700 K stable over 10 h for NRIXS studies were achieved. From the NRIXS spectrum, the absolute temperature of the sample can be determined by the detailed balance of the energy spectrum. This provides independent determination of the sample temperature besides the spectral radiometric method commonly used in LHDAC experiments. More importantly, this method is useful for temperatures below 1000 K, where the spectral radiometric method is limited owing to weak thermal emission.

A future upgrade of the LHDAC system includes the possibility to measure temperature from both sides of the DAC, either by using two spectrographs or by guiding both upstream and downstream beams to different areas of the CCD in a spectrograph system. A ‘cleanup’ slit [19] between the KB mirror and the DAC could be helpful to obtain a sharper X-ray focusing spot for simultaneous X-ray diffraction studies.

Intrinsically, NRIXS is a low count rate experiment. Current experiments typically took 4–10 h to collect sufficiently accurate energy spectra, depending on the concentration of the  $^{57}\text{Fe}$  isotope in the sample. Obviously, an increase in photon flux will be beneficial for such measurements. A combination of focusing device with increased efficiency and improved insertion devices with shorter magnetic period and increased length can provide us with a fivefold intensity gain the near future.

## Acknowledgements

We thank J. Burke, V. Prakapenka, D. Errandonea, S.-K. Lee, M. Hu, D. Hauserman, M. Yue, M.L. River, S. Hardy, V.V. Struzhkin, D. L. Heinz, G. Steinle-Neumann, R. Cohen, and J. M. Jackson, for their help during our LHDAC system construction and testing. Use of the advanced photon source is supported by the U.S. Department of Energy, Office of Basic Energy Sciences, Office of Science, under contract no. W-31-109-ENG-38. Work at Carnegie was supported by DOE/BES, DOE/NNSA (CDAC# DE-FC03-03NA00144), NASA, NSF, and the W.M. Keck Foundation.

## References

- [1] M. Seto, Y. Yoda, S. Kikuta, X. Zhang and M. Ando, Observation of nuclear resonant scattering accompanied by phonon excitation using synchrotron radiation, *Phys. Rev. Lett.*, **74**, 3828 (1995).
- [2] W. Sturhahn, T. Toellner, E. Alp, X. Zhang, M. Ando, Y. Yoda, S. Kikuta, M. Seto, C. Kimball and B. Davrowski, Phonon density of states measured by inelastic nuclear resonant scattering, *Phys. Rev. Lett.*, **74**, 3832 (1995).
- [3] E. E. Alp, W. Sturhahn and T. Toellner, Synchrotron Mossbauer spectroscopy of powder samples, *Nucl. Instrum. Meth. B*, **97**, 526 (1995).
- [4] H. K. Mao, J. Xu, V. V. Struzhkin, J. Shu, R. J. Hemley, W. Sturhahn, M. Y. Hu, E. E. Alp, L. Vocadlo, D. Alfè, G. D. Price, M. J. Gillan, M. Schwoerer-Böhning, D. Häusermann, P. Eng, G. Shen, H. Giefers, R. Lübbbers and G. Wortmann, Phonon density of states of iron up to 153 gigapascals, *Science*, **292**, 914 (2001).

- [5] J. Zhao, T. Toellner, M. Hu, W. Sturhahn and E. Alp, High energy-resolution monochromator for 83Kr nuclear resonant scattering, *Rev. Sci. Instrum.*, **73**, 1608 (2002).
- [6] J. Jackson, W. Sturhahn, G. Shen, J. Y. Zhao, M. Hu, D. Errandonea, J. Bass and Y. Fei, (Mg,Fe)SiO<sub>3</sub> perovskite up to 120 GPa using synchrotron Mössbauer spectroscopy, *Am. Mineral.*, (2004), in press. Q1
- [7] E. Gerdau and H. de Waard (ed.), Nuclear resonant scattering of synchrotron radiation, *Hyperfine Interact.*, 123–125 (1999/2000).
- [8] W. Sturhahn, Nuclear resonant spectroscopy, *J. Phys. – Condens. Matter*, **16**, 497 (2004).
- [9] G. Shen, W. Sturhahn, E. E. Alp, J. Zhao, T. S. Toellner, V. B. Prakapenka, Y. Meng and H. K. Mao, Phonon density of states in iron at high pressures and high temperatures, *Phys. Chem. Miner.*, **31**, 353 (2004).
- [10] J. Lin, V. Struzhkin, W. Sturhahn, E. Huang, J. Y. Zhao, M. Hu, E. Alp, H. Mao, N. Boctor and R. Hemley, Sound velocities of iron-nickel and iron-silicon alloys at high pressure, *Geophys. Res. Lett.*, **30**, 2112 (2003).
- [11] J. F. Lin, Y. Fei, W. Sturhahn, J. Y. Zhao, H. K. Mao and R. J. Hemley, Magnetic transition and sound velocities of Fe<sub>3</sub>S at high pressure, *Earth Planet. Sci. Lett.*, (2004), in press. Q1
- [12] L. C. Ming and W. A. Bassett, Laser heating in the diamond anvil press up to 2000 °C sustained and 3000 °C pulsed at pressures up to 260 kilobars, *Rev. Sci. Instrum.*, **45**, 1115 (1974).
- [13] W. A. Bassett, The birth and development of laser heating in diamond anvil cells, *Rev. Sci. Instrum.*, **72**, 1270 (2001).
- [14] G. Shen, V. B. Prakapenka, M. L. Rivers and S. R. Sutton, Structure of liquid iron at pressures up to 58 GPa, *Phys. Rev. Lett.*, **92**, 185701 (2004).
- [15] R. Boehler and A. Chopelas, A new approach to laser heating in high pressure mineral physics, *Geophys. Res. Lett.*, **18**, 1147 (1991).
- [16] P. Lazor, G. Shen and S. K. Saxena, Laser-heated diamond anvil cell experiments at high pressure: melting curve of nickel up to 700 kbar, *Phys. Chem. Miner.*, **20**, 86 (1983).
- [17] A. Dewaele, G. Fiquet, D. Andraut and D. Hausermann, P-V-T equation of state of periclase from synchrotron radiation measurements, *J. Geophys. Res.*, **105**, 2869 (2000).
- [18] G. Shen, H. K. Mao, R. J. Hemley, T. S. Duffy and M. L. Rivers, Melting and crystal structure of iron at high pressures and temperatures, *Geophys. Res. Lett.*, **25**, 373 (1998).
- [19] G. Shen, M. L. Rivers, Y. Wang and S. R. Sutton, Laser heated diamond cell system at the advanced photon source for *in situ* X-ray measurements at high pressure and temperature, *Rev. Sci. Instrum.*, **72**, 1273 (2001).
- [20] J. F. Lin, M. Santoro, V. V. Struzhkin, H. K. Mao and R. J. Hemley, *In situ* high pressure-temperature Raman spectroscopy technique with laser-heated diamond anvil cells, *Rev. Sci. Instrum.*, in press. Q1
- [21] J. F. Lin, W. Sturhahn, J. Zhao, G. Shen, H. Mao and R. Hemley, Absolute temperature measurement in a laser-heated diamond anvil cell, *Geophys. Res. Lett.*, **31**, L14611 (2004).
- [22] T. Toellner, Monochromatization of synchrotron radiation for nuclear resonant scattering experiments, *Hyperfine Interact.*, **125**, 3 (2000).
- [23] T. Toellner *et al.* (to be published). Q1
- [24] P. J. Eng, M. Newville, M. L. Rivers and S. R. Sutton, *Proc. SPIE*, **3449**, 145 (1998).
- [25] D.L. Heinz and R. Jeanloz, Temperature measurements in the laser-heated diamond cell, In: *High-Pressure Research in Mineral Physics*, edited by M. H. Manghnani, and Y. Syono, terra Scientific Publishing Company (TERRAPUB), Tokyo/American Geophysical Union, Washington, D.C., (1987), 113.
- [26] W. Sturhahn and V. G. Kohn, Theoretical aspects of incoherent nuclear resonant scattering, *Hyperfine Interact.*, **123/124**, 367 (1999).



**Taylor & Francis**  
Taylor & Francis Group

**Journal... High Pressure Research**

**Article ID... GHPR041040**

**TO: CORRESPONDING AUTHOR**

**AUTHOR QUERIES - TO BE ANSWERED BY THE AUTHOR**

The following queries have arisen during the typesetting of your manuscript. Please answer the queries.

Q1	Please update the references 6, 11, 20, 23.	

Production Editorial Department, Taylor & Francis Ltd.  
4 Park Square, Milton Park, Abingdon OX14 4RN

Telephone: +44 (0) 1235 828600

Facsimile: +44 (0) 1235 829000